Neuron
Article

Cholinergic Enhancement Reduces Spatial Spread of Visual Responses in Human Early Visual Cortex

Michael A. Silver,[1,2,3,*] Amitai Shenhav,[1,2,3] and Mark D'Esposito[2,3]
[1]School of Optometry, University of California, Berkeley, Berkeley, CA 94720, USA
[2]Helen Wills Neuroscience Institute, University of California, Berkeley, Berkeley, CA 94720, USA
[3]Henry H. Wheeler, Jr. Brain Imaging Center, University of California, Berkeley, Berkeley, CA 94720, USA
*Correspondence: masilver@berkeley.edu
DOI 10.1016/j.neuron.2008.09.038

SUMMARY

Animal studies have shown that acetylcholine decreases excitatory receptive field size and spread of excitation in early visual cortex. These effects are thought to be due to facilitation of thalamocortical synaptic transmission and/or suppression of intracortical connections. We have used functional magnetic resonance imaging (fMRI) to measure the spatial spread of responses to visual stimulation in human early visual cortex. The cholinesterase inhibitor donepezil was administered to normal healthy human subjects to increase synaptic levels of acetylcholine in the brain. Cholinergic enhancement with donepezil decreased the spatial spread of excitatory fMRI responses in visual cortex, consistent with a role of acetylcholine in reducing excitatory receptive field size of cortical neurons. Donepezil also reduced response amplitude in visual cortex, but the cholinergic effects on spatial spread were not a direct result of reduced amplitude. These findings demonstrate that acetylcholine regulates spatial integration in human visual cortex.

INTRODUCTION

The neurotransmitter acetylcholine (ACh) has been implicated in a variety of cognitive processes, including learning and memory (Hasselmo, 2006) and attention (Sarter et al., 2005). The physiological effects of ACh in the brain have typically been investigated in animal experiments, while behavioral effects have been extensively characterized by administering cholinergic drugs to human subjects. However, little is known regarding the physiological effects of ACh in the human brain. We manipulated synaptic ACh levels by administering the Alzheimer's disease medication and cholinesterase inhibitor donepezil (trade name: Aricept) to healthy human subjects. Donepezil enhances cholinergic synaptic transmission in the brain by inhibiting the enzyme that metabolizes ACh in the synaptic cleft, thereby prolonging the effective lifetime of this neurotransmitter. The effects of cholinergic enhancement on responses to visual stimuli in visual cortex were assessed using functional magnetic resonance imaging (fMRI).

A number of experiments have provided evidence that, in cerebral cortex, ACh increases thalamocortical synaptic transmission relative to lateral intracortical connections (reviewed in Giocomo and Hasselmo, 2007). Other studies have demonstrated a role for ACh in the regulation of spatial integration of activity within visual cortex. ACh reduced spread of excitatory activity following electrical stimulation of rat visual cortical slices (Kimura et al., 1999) and decreased the preferred length of visual stimuli in marmoset V1 neurons (Roberts et al., 2005).

A shift in the balance of cortical inputs by ACh in favor of thalamocortical relative to intracortical inputs would be expected to decrease excitatory receptive field (RF) size, as the size of the classical RF, or minimum response field, is thought to be largely determined by thalamocortical inputs, while the excitatory portion of the surrounding extraclassical RF is due mainly to intracortical connections (Angelucci and Bressloff, 2006). Based on the animal physiology studies, ACh would suppress the intracortical inputs that give rise to the extraclassical RF relative to the feedforward thalamocortical inputs that are responsible for the classical RF. This would result in a reduction in overall excitatory RF size. We hypothesized that if enhancing cholinergic transmission with donepezil decreased excitatory RF size of a large population of visual cortical neurons in the human brain, this would reduce the spatial spread of excitatory visual responses within visual cortex. In this context, a reduced spatial spread of visual responses can be seen as a shift in the responsiveness of cortex toward feedforward inputs and away from local intrinsic processing.

We employed a combination of retinotopic mapping of early visual cortical areas, representation of the spatial spread of visual responses on computationally flattened patched of visual cortex, and a novel analysis method to quantify spatial spread of excitatory visual responses within the cortical gray matter. In agreement with the hypothesis outlined above, we found that increasing cholinergic transmission with donepezil reduced spatial spread of excitatory visual responses in human early visual cortex.

RESULTS

Functional MRI (fMRI) was used to measure the spatial spread of visual responses in early visual cortex and modulation of this spatial spread by cholinergic enhancement. Subjects passively viewed a high-contrast, contrast-reversing checkerboard

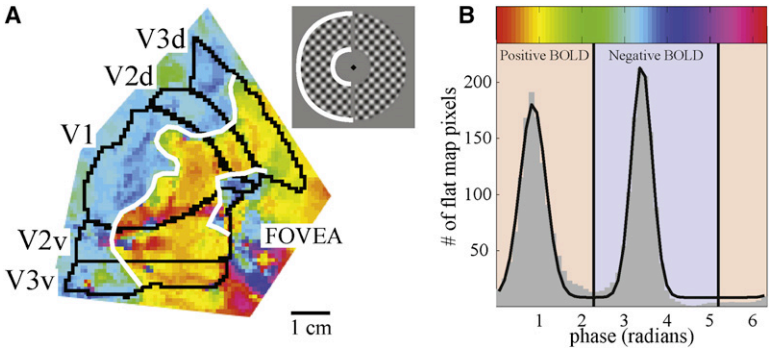

Figure 1. Responses to Visual Stimulation Have a Bimodal Phase Distribution in Early Visual Cortex

A checkerboard annulus stimulus was presented in block alternation with a gray screen. A sinusoid with a frequency equal to the frequency of block alternation (0.0521 Hz) was fit to the fMRI time course of each pixel in a computationally flattened patch of early visual cortex. The phase of this sinusoid relative to the stimulus cycle was color coded according to the color map above panel (B) and plotted on the flat map of the right hemisphere of subject #4. No spatial smoothing or statistical thresholding was performed.

(A) Spatial distribution of response phases in cortical areas V1, V2, and V3. The shape of half of the stimulus annulus can be seen in the pattern of responses in early visual cortex. Due to the contralateral organization of the visual pathways, the left side of the stimulus annulus is represented in this right hemisphere flat map. At the foveal confluence and in regions representing peripheral visual field locations, the phases are mainly blue, consistent with a negative BOLD (inhibitory) response to the stimulus. In between, the phases are mainly yellow and orange, consistent with a positive BOLD response. Average data are shown here to demonstrate the spatial distribution of positive and negative BOLD responses, but all the quantitative analysis of donepezil effects was performed on single 5 min fMRI runs without averaging. The borders between the positive and negative BOLD responses are indicated by white lines and correspond to the inner and outer boundaries of half of the stimulus annulus.

(B) Pixel histogram of the data shown in panel (A). The distribution of response phases was bimodal, with one mode corresponding to positive BOLD responses and the other corresponding to negative BOLD responses. This phase distribution was well fit by the two-Gaussian model.

annulus in block alternation with a blank gray screen while maintaining fixation on a central point. A sinusoid with a period equal to that of the block alternation (19.2 s) was fit to the fMRI time series of each voxel in retinotopically mapped visual cortical areas V1, V2, and V3. The free parameters of the sinusoidal fit were amplitude (corresponding to the magnitude of the visually driven response) and phase (corresponding to the temporal delay of the response relative to the stimulus block alternation). Amplitude and phase values were displayed on computationally flattened patches of visual cortex.

The spatial distribution of response phases on the cortical surface was consistent with the known retinotopic organization of early visual cortical areas. Positive BOLD responses to the checkerboard stimulus relative to the gray screen were observed in V1, V2, and V3 at visual field locations corresponding to the eccentricities of the stimulus annulus (Figure 1A). Negative BOLD responses (stimulus caused a decrease in response relative to the gray screen) were observed both peripheral and central to the positive BOLD region (Figure 1A). These negative BOLD responses extended into the foveal confluence and peripherally for a few centimeters beyond the retinotopic representation of the outer boundary of the stimulus annulus.

The response phase values for all the pixels in each hemisphere of each visual area were displayed as a histogram (Figure 1B). This histogram was bimodal, with one mode corresponding to the positive BOLD response to the stimulus and the other mode containing pixels with negative BOLD responses (Figure 1B). The histograms were fit with two Gaussians, one for each mode. The crossing points of the two Gaussians were used to define the phase boundaries that distinguished positive BOLD from negative BOLD responses. The spatial spread of the excitatory visual response was defined as the fraction of pixels within the positive BOLD region of the phase histogram.

The hemodynamic response function (HRF) describes the relationship between neural activity and the BOLD response. Specifically, the BOLD response is delayed and temporally low-pass filtered relative to the time course of neural activity. If the first peak of the pixel histogram shown in Figure 1B represents an excitatory response to visual stimulation, then the average fMRI time course from pixels in this phase window should closely match a convolution of the expected neural activity time series and the HRF. This is exactly the result that was obtained (Figure 2A). Similarly, pixels comprising the second peak of the phase histogram exhibited a BOLD time course consistent with a decrease in neural activity during stimulus presentation (Figure 2B).

The cholinesterase inhibitor and Alzheimer's disease medication donepezil (trade name: Aricept) was administered to increase synaptic levels of ACh. Donepezil reduced the spatial spread of the excitatory visual response. That is, the positive BOLD response to the stimulus occupied less of the cortical surface following cholinergic enhancement with donepezil (Figure 3). Mean pixel phase histograms and binarized cortical flat maps for individual subjects are presented as Supplemental Data. The histograms all exhibit a bimodal distribution of response phases corresponding to positive and negative BOLD responses to the visual stimulus (Figure S1). Additionally, the binarized flat maps show that the spatial distributions of the pixels with positive BOLD responses correspond to the retinotopic representation of the stimulus in early visual cortex, while more peripheral visual field representations contain pixels with negative BOLD responses (Figure S2). Figure 2C displays the average responses for pixels that were classified as having a positive BOLD response under placebo and a negative BOLD response under donepezil. These two sinusoidal time courses are 180° out of phase with respect to each other, demonstrating that the pixel classification procedure used to measure spatial spread identifies a population of visual cortical pixels that change their response to visual stimulation from positive to negative following cholinergic enhancement with donepezil.

For the group of five subjects, the effects of cholinergic enhancement on spatial spread were significant in areas V1 and

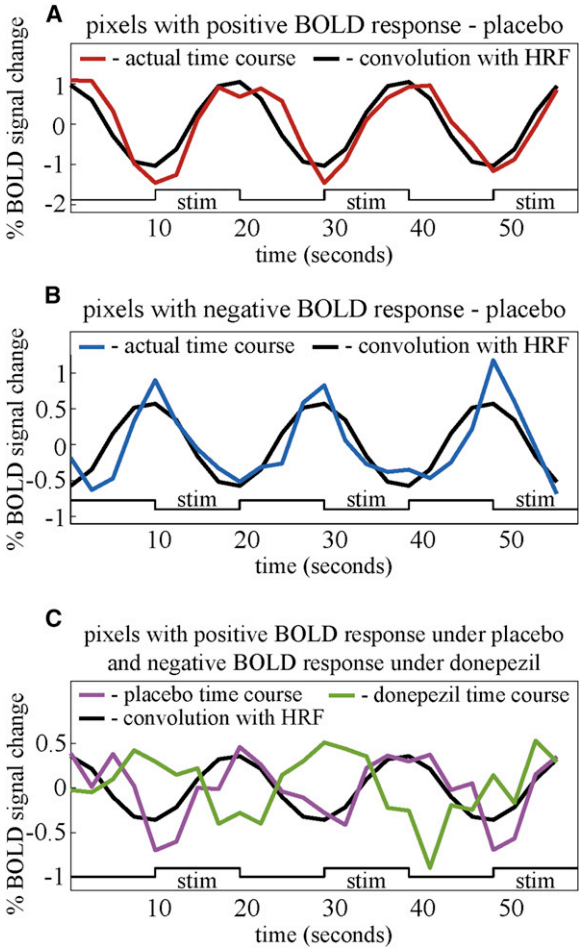

Figure 2. Correlation of fMRI Time Courses with Models Based on Expected Time Courses of Neural Activity

(A) Step function at the bottom indicates the timing of stimulus presentation and the expected time course of activity for neurons excited by the stimulus. Black line, convolution of this step function with a canonical hemodynamic response function (HRF). Red line, actual mean fMRI time series from pixels in the positive BOLD phase window in the histogram shown in Figure 1B. The actual and modeled time courses are very similar.

(B) Step function shows expected response for neurons that are inhibited by stimulus presentation. Black line, convolution of this step function with the HRF. Blue line, mean fMRI time series from pixels in the negative BOLD phase window in the histogram in Figure 1B. Again, the two curves are similar. In addition, they are both 180° out of phase relative to the positive BOLD responses shown in panel (A).

(C) Step function as in panel (A). Black line, convolution of step function with the HRF. The purple and green lines are average fMRI time series from the population of pixels that were classified as having a positive BOLD response under placebo (red in left panel of Figure 3) and a negative BOLD response under donepezil (blue in right panel of Figure 3). This demonstrates that the same population of pixels can respond either positively (purple) or negatively (green), depending on the level of cholinergic enhancement.

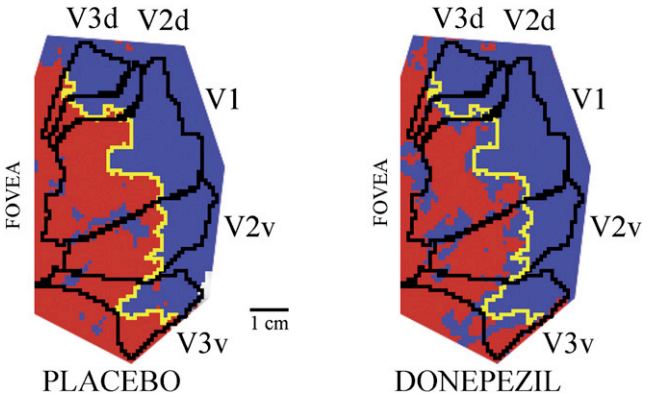

Figure 3. The Spatial Spread of the Positive BOLD Response to Visual Stimulation Is Reduced following Donepezil Administration

Each cortical flat-map pixel in the left hemisphere of subject #4 was assigned a color based on the phase of its response relative to the stimulus cycle. Red, pixels with a positive BOLD (excitatory) response to the checkerboard stimulus. Blue, pixels with a negative BOLD (inhibitory) response. Yellow, boundary between the positive BOLD region and the surrounding negative BOLD region, drawn based on the placebo condition. Donepezil reduced the number of pixels with a positive BOLD response and increased the number of pixels with a negative BOLD response to the stimulus.

V3 but not V2 (Figure 4). In areas V1 and V3, the reduction in spatial spread relative to placebo was 8.5% and 7.3%, respectively, corresponding to a decrease in visual space of ~0.4° of visual angle. Inspection of individual flat maps revealed that a single donepezil fMRI session of subject #5 was unlike all the other sessions in that donepezil caused a substantial (15%) increase in excitatory spatial spread that was limited to a single cortical area (V2). We do not currently have an explanation for this finding, but the fact that this single session produced unusual results in V2 but not in neighboring cortical areas V1 and V3 suggests that this session may have been contaminated by an imaging artifact. If this aberrant session is excluded (representing 4 out of a total of 84 fMRI runs), the effects of donepezil on excitatory spatial spread are much more consistent across the three visual areas. The consequences of excluding this session on subject #5′s mean pixel histograms (Figure S1), subject #5′s binarized flat maps (Figure S2), and on the spatial spread bar graphs for subject #5 and the entire group of five subjects (Figure S3) are included as Supplemental Data. Analysis of the spatial spread results following exclusion of the aberrant session indicated a statistically significant reduction in spatial spread following donepezil administration in all three visual cortical areas. Cholinergic enhancement also reduced the amplitude of the visually evoked positive BOLD response in areas V1, V2, and V3 (Figure 4) and increased the amplitude of the negative BOLD response in V1 (Figure S4).

In conventional statistical parametric mapping analyses of BOLD responses, spatial spread and response amplitude are usually confounded. Typically, a statistical threshold is chosen, and voxels with t statistic values that exceed the threshold are displayed and analyzed. Any manipulation that reduces response amplitude will also reduce the signal-to-noise ratio of the response. This will result in fewer suprathreshold voxels and an apparent decrease in the spatial extent of the activated region (Saad et al., 2003). In contrast, the analysis we employed assigns a phase to every pixel in the flat map, regardless of the amplitude or reliability of the response. Each pixel is included

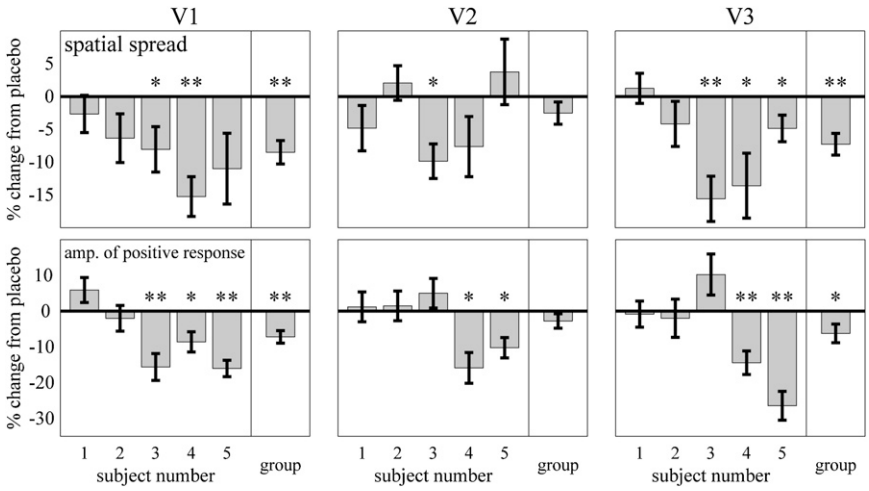

Figure 4. Donepezil Reduced Spatial Spread and Amplitude of Excitatory Visual Responses in Early Visual Cortex

For each 5 min fMRI run, a phase histogram like that shown in Figure 1B was generated and fit with the two-Gaussian model. This allowed the categorization of each pixel as either positive or negative BOLD. The fraction of positive BOLD responses was computed separately for left and right hemispheres in each visual area. In addition, the amplitude of the best-fit sinusoid was computed for each pixel that was classified as having a positive BOLD response to the stimulus. Error bars are SEM. *$p < 0.05$; **$p < 0.001$.

in the phase histogram and contributes equally to the two-Gaussian fit, thereby avoiding the "iceberg" problem created by statistical thresholding. Nevertheless, we directly tested whether the reduction in spatial spread caused by donepezil could artifactually result from the effects of cholinergic enhancement on response amplitude. For each 5 min run, we correlated the change in magnitude of the positive BOLD response following donpezil administration with the drug-induced change in positive BOLD spatial spread. These measures were not significantly correlated in any of the three visual areas (Figure 5).

Because the subjects differed in both mean and variance of the effects of donepezil on spatial spread and amplitude of positive BOLD responses (Figure 4), pooling all the data across subjects could have obscured a possible correlation between these two measures. To test this directly, we computed z scores for the percent change in spatial spread and positive amplitude values relative to placebo and correlated these two sets of standardized z scores. They were not significantly correlated in any area (correlation coefficients: −0.07 in V1, 0.11 in V2, and −0.11 in V3). Therefore, even though donepezil generally reduced both spatial spread and amplitude of positive BOLD visual cortical responses, the decrease in spatial spread was not directly due to a reduction in response amplitude.

The BOLD signal measured with fMRI can be modulated by alterations in neural activity as well as changes in neurovascular coupling or the vasculature itself. Breath holding elevates BOLD signals in the cortex (Stillman et al., 1995) by causing hypercapnia that results in vascular dilation and increased blood flow (Li et al., 1999). We tested whether donepezil had any effect on the breath holding BOLD response. Subjects alternated blocks of breath holding with paced breathing. This generated sinusoidal modulation of BOLD signal over the entire cerebral cortex. The mean amplitudes and response phases of the sinusoidal fits for each gray matter voxel were computed for areas V1, V2, and V3. Donepezil produced no significant differences in amplitude, but it reduced the response phase (temporal delay) of the breath holding response in areas V1 and V3 (Figure 6). These changes in the temporal properties of the BOLD response would not be expected to have important consequences for the measurement of spatial spread of visual responses. A decrease in response delay would shift the phase values in the pixel histograms toward lower values (Figure 1B), but presumably the bimodal distribution and the assignment of each pixel to either the positive or negative BOLD mode would be largely unaffected.

We also measured the effects of donepezil on the other free parameters of the two-Gaussian fit of the visually evoked response phase pixel histogram. These included means of the Gaussians (corresponding to the temporal delays of the positive and negative BOLD responses relative to the stimulus cycle), the standard deviations of the Gaussians (corresponding to the widths of the peaks in the pixel histogram), and a y-offset term (modeled as a constant value that was added to all bins of the pixel histogram). In general, cholinergic enhancement had fairly minimal effects on these measures, although there was a consistent increase in the value of the y-offset term in all three visual

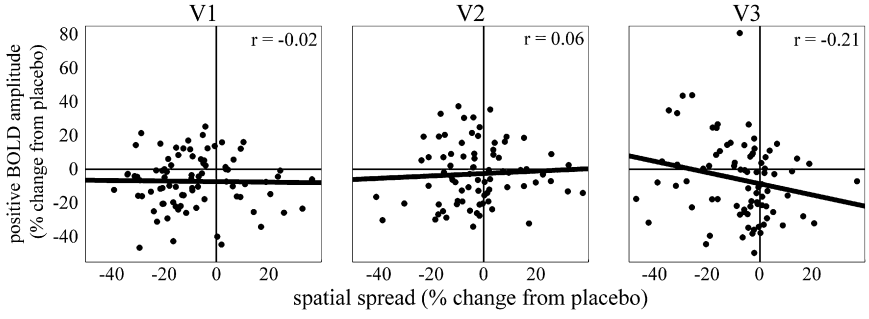

Figure 5. The Effects of Donepezil on Spatial Spread and on the Amplitude of Excitatory Visual Responses Were Uncorrelated

For each fMRI run in the donepezil sessions, the proportion of positive BOLD pixels (spatial spread) and the response amplitude of these positive BOLD pixels were measured and normalized by the corresponding mean values in the placebo condition.

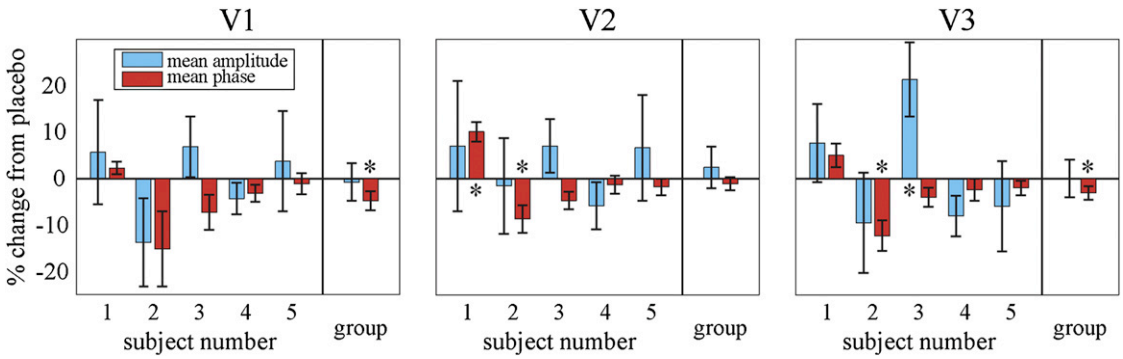

Figure 6. Effects of Donepezil on the BOLD Response to Breath Holding

Subjects alternated blocks of breath holding and paced breathing, and a sinusoid with a period equal to the period of block alternation (48 s) was fit to the fMRI time series for each visual cortical flat-map pixel. The mean response amplitude (blue) and phase (red, corresponding to the temporal delay of the BOLD response) are shown. For the group of five subjects, donepezil had no effect on mean amplitude and decreased mean phase relative to placebo in areas V1 and V3. Error bars are SEM. *$p < 0.05$.

areas following donepezil administration (Figures S5–S7). In addition, there was no effect of donepezil on the mean squared error, an estimate of the goodness-of-fit of the two-Gaussian model (Figure S8).

Finally, we measured the effects of cholinergic enhancement on visual fixation stability. In principle, changes in fixation stability following donepezil administration could result in artifactual alterations of spatial spread. Deviations from fixation would cause the visual stimulus to activate a larger portion of the retina over an entire fMRI run. While the precise consequences of this for spatial spread measurements would depend on the temporal properties of the eye movements, it is nevertheless a potential confound. We measured the effects of donepezil on fixation stability for four of the five subjects who participated in the fMRI experiments. Eye position was measured in a behavioral testing room outside the scanner. The pharmacological procedures and checkerboard annulus stimulus were identical to those used in the fMRI experiments.

Table 1. Donepezil Had Minimal Effect on Fixation Stability during Passive Viewing of the Checkerboard Stimulus Annulus

	Placebo			Donepezil		
Subject #	SD_x (deg)	SD_y (deg)	% Fix Wind.	SD_x (deg)	SD_y (deg)	% Fix Wind.
2	0.34	0.29	78	0.59	0.89	56
3	0.26	0.32	98	0.34	0.39	89
4	0.38	0.35	94	0.34	0.27	97
5	0.66	0.56	91	0.63	0.42	93
Group	0.41	0.38	90	0.47	0.49	84

Subjects #2 to #5 from the fMRI portion of this study repeated the passive viewing experiment in a behavioral testing room. The pharmacological procedures and visual stimulus were identical to those used in the fMRI experiments. Time series of horizontal (x) and vertical (y) position were recorded, and the standard deviation (SD_x and SD_y) over each 5 min run was computed. Standard deviations are presented in units of degrees of visual angle. In addition, a circular fixation window of 1° radius was defined, and the percent of viewing time during which the eye position was within this window was measured. None of the three eye position measures showed significant differences between placebo and donepezil sessions (paired t test).

The most direct measure of fixation stability is the standard deviation of eye position. This was measured for both horizontal and vertical eye position (Table 1). We also computed the percentage of time that subjects successfully maintained eye position within a 1° radius circular window centered at fixation. In general, the subjects maintained fixation very effectively. The standard deviations of the eye position traces were small (averaging less than 0.5° of visual angle), and the eye position was within 1° of the fixation point for a substantial portion of time (averaging more than 85%). Most importantly for this study, there was no consistent effect of cholinergic enhancement with donepezil on fixation stability. Subjects #2 and #3 had more stable fixation for placebo than for donepezil, while subjects #4 and #5 showed the opposite effect. These results provide strong evidence against a role for eye movements in the observed effects of donepezil on excitatory spatial spread in visual cortex.

Cholinergic synapses in the eye regulate pupil size, and chronic daily administration of 5 mg donepezil to patients with Alzheimer's disease reduced pupil size by 7% (Estermann et al., 2006). If acute administration of donepezil decreased pupil size in our study, this would have reduced the overall amount of light reaching the retina. However, luminance adaptation renders many neurons in the visual system fairly insensitive to small and slow changes in overall light levels. Therefore, it is unlikely that the effects of donepezil on excitatory spatial spread of responses in visual cortex are due to changes in pupil size.

DISCUSSION

Relation to Previous Studies

We have shown that increasing synaptic ACh levels reduces the spatial spread of excitatory visual responses in human early visual cortex. Measurement of spatial spread of responses with fMRI reflects the activity of large populations of visual cortical neurons. The most direct analog of this measure in single-unit electrophysiology studies is the excitatory receptive field (RF) size of visual cortical neurons. Indeed, local iontophoresis of

ACh has been reported to reduce the preferred length of visual stimuli in marmoset V1 neurons (Roberts et al., 2005). Additionally, in slices of rat visual cortex, bath application of ACh reduced the spread of excitation following electrical stimulation at the white matter/layer VI border, as measured with voltage-sensitive optical imaging (Kimura et al., 1999).

The size and spatial organization of V1 RFs result from a combination of feedforward inputs from the lateral geniculate nucleus (LGN), lateral connections from other V1 neurons, and feedback projections from extrastriate areas (reviewed in Angelucci and Bressloff, 2006). The classical receptive field (CRF), or minimum response field, for a given neuron corresponds to the visual field locations where presentation of small optimal stimuli evokes an excitatory response in that neuron. The spatial extent of the CRF of a given V1 neuron closely matches the visuotopic extent of the LGN neurons that project to that cell (Angelucci and Sainsbury, 2006). For many visual cortical neurons, increasing the size of the visual stimulus reveals the presence of an additional excitatory component of the RF that surrounds the CRF, known as the summation receptive field, or SRF. Further increases in stimulus size beyond the SRF often result in a decrease in the magnitude of visual responses, or surround suppression (Hubel and Wiesel, 1965; DeAngelis et al., 1994; Sceniak et al., 1999; Cavanaugh et al., 2002). The spatial extent of the SRF of a given V1 cell is very similar to the visuotopic extent of the V1 neurons that project to that cell through lateral connections (Angelucci et al., 2002). Taken together, these results suggest that the center of a V1 receptive field (the CRF) corresponds mainly to feedforward inputs from the LGN, while the surrounding portions of the excitatory receptive field (the SRF) are associated primarily with lateral intracortical connections.

One possible mechanism to account for the reduction in spatial spread in visual cortex by ACh is a shift in the balance of feedforward and lateral synaptic transmission. In general, pharmacological enhancement of cholinergic activity boosts afferent inputs relative to intracortical connections. This was first shown in rat piriform cortex, which exhibits a laminar segregation of afferent inputs and excitatory intrinsic fibers (Hasselmo and Bower, 1992). In neocortex, electophysiological recordings have shown that ACh enhances thalamocortical relative to intracortical transmission in brain slices (Gil et al., 1997; Hsieh et al., 2000) and in vivo (Disney et al., 2007; Metherate and Ashe, 1993; Oldford and Castro-Alamancos, 2003). The results of Kimura et al. (1999) are also consistent with this, as ACh caused less suppression of excitatory spatial spread in the thalamocortical-recipient layer IV compared to superficial or deep cortical layers.

A shift in the balance of cortical inputs by ACh in favor of thalamocortical relative to intracortical inputs in human visual cortex would be expected to enhance the CRF relative to the SRF, resulting in a decrease in excitatory RF size. At the population level, reduction of excitatory receptive field size over many neurons should reduce excitatory spatial spread, as we have observed with fMRI.

Simultaneous electrophysiological and fMRI recordings in macaque visual cortex have demonstrated that local field potential (LFP) signals more effectively predict the BOLD response than multiunit spiking activity (MUA) (Logothetis et al., 2001). To the extent that fMRI signals should be considered to represent synaptic inputs and subthreshold processing rather than spiking activity in a given area, this would call into question our interpretation of the fMRI spatial spread results in terms of receptive fields of individual visual cortical neurons. However, both LFP and MUA signals are highly correlated with the BOLD signal, and the differences between their correlations with the BOLD signal are small (Logothetis et al., 2001). Additionally, LFP and MUA responses to visual stimulation have been reported to be equally well-correlated with BOLD responses in cat visual cortex, providing that activity is integrated over at least several millimeters of cortex (Kim et al., 2004). Our spatial spread measures typically include hundreds of square millimeters of cortex in a given visual area.

Finally, recordings of MUA, LFP, and BOLD responses to visual stimulation in macaque V1 demonstrated that the electrophysiological signals increased in regions exhibiting a positive BOLD response and decreased in regions with a negative BOLD response (Shmuel et al., 2006). Also, the MUA and LFP signals were equally well correlated with the negative BOLD response in this study. Thus, the available evidence, at least in early visual cortex, supports a strong relationship between spiking activity in visual cortical neurons and fMRI responses in these areas.

Possible Sites of Action of Cholinergic Enhancement

Donepezil and other cholinesterase inhibitors prolong the lifetime of ACh in the synaptic cleft by blocking the enzyme that metabolizes ACh. Manipulation of the cholinergic system with cholinesterase inhibitors is more physiologically relevant than using ACh receptor agonists or antagonists. Receptor agonists and antagonists interact directly with particular receptor subtypes and alter cholinergic activity at all synapses where those receptor subtypes are located, independent of the endogenous activity at those synapses during the response to the stimulus or performance of the relevant task. In contrast, cholinesterase inhibition enhances cholinergic activity only at synapses where ACh is currently being endogenously released. It therefore amplifies the effects of ACh at those cholinergic synapses that are active during the experimental manipulation of interest.

A disadvantage of cholinesterase inhibitors is that they do not provide information regarding the ACh receptor subtypes that might be mediating their effects. In the present study, donepezil could be acting on any of the following ACh receptor populations: presynaptic nicotinic receptors on thalamocortical afferents in layer IV (Prusky et al., 1987; Disney et al., 2007), muscarinic receptors on cortical neurons (Levey et al., 1991), or nicotinic receptors on thalamocortical axons (located on the portion of the axon proximal to the presynaptic terminals) (Kawai et al., 2007).

In addition, cholinergic enhancement could be affecting top-down inputs to early visual cortex. Basal forebrain cholinergic axons project to the hippocampus and the entire cerebral cortex (Mesulam, 2004). A number of studies have demonstrated changes in fMRI activity in human brain areas outside of visual cortex following administration of cholinergic drugs. The muscarinic receptor antagonist scopolamine reduced the extent and magnitude of encoding-related fMRI responses in the hippocampus, fusiform gyrus, and inferior prefrontal cortex (Sperling

et al., 2002) and decreased sustained fMRI signals associated with long-term encoding in parahippocampal and hippocampal regions (Schon et al., 2005). Additionally, the cholinesterase inhibitor physostigmine has been shown to modulate top-down visual working memory (Furey et al., 2000) and visual spatial attention signals (Bentley et al., 2004; Bentley et al., 2008) There are many examples of cholinergic regulation of visual attention in both humans and animal models (Hasselmo and McGaughy, 2004; Sarter et al., 2005). Future studies that directly compare attentional and pharmacological modulation of visual responses will clarify the possible role of top-down attention on excitatory spatial spread. Interestingly, top-down attention has been reported to have similar effects to ACh on spatial integration of individual macaque V1 neurons. Specifically, allocation of spatial attention to a visual field location within the recorded neuron's receptive field reduced receptive field size at parafoveal (but not peripheral) eccentricities (Roberts et al., 2007).

Cholinergic Effects on Response Amplitude

In the present study, donepezil reduced the amplitude of excitatory visual responses in visual cortex. Jacobsen et al. (2002) reported no effect of intravenous nicotine administration on visually-evoked BOLD responses in occipital cortex, and the muscarinic receptor antagonist scopolamine did not alter either the response magnitude or spatial extent of visual cortical fMRI responses (Sperling et al., 2002). In addition, the cholinesterase inhibitor physostigmine did not affect regional cerebral blood flow (rCBF) responses to visual stimulation in Brodmann's area 17 (calcarine cortex) as measured with positron emission tomography, but it did increase rCBF in Brodmann's area 19 (middle occipital gyrus) (Mentis et al., 2001). Physostigmine has also been reported to reduce visual responses in the calcarine sulcus (corresponding to early visual cortex) but not in lateral occipital cortex (Bentley et al., 2004).

Some of the heterogeneity in these results may be due to the fact that response amplitude has often been confounded with spatial spread in these studies. In addition, these studies generally modeled only positive responses to visual stimulation. In the present study, both positive BOLD and negative BOLD responses to visual stimulation were observed in the same cortical area. We employed retinotopic mapping to identify the boundaries of V1, V2, and V3 and used gray-matter segmentation and flat mapping in order to visualize the spatial extent of the positive and negative BOLD responses in each area. In addition, we did not perform any statistical thresholding of fMRI responses, so we were able to independently measure the effects of cholinergic enhancement on spatial spread and on response amplitude. These novel analysis methods showed that donepezil reduced the number of positive BOLD pixels in early visual cortex as well as the amplitude of excitatory visual responses in these pixels.

Local administration of ACh to visual cortex of anesthetized animals has produced variable results. ACh has been reported to increase visual responses (Sato et al., 1987; Sillito and Kemp, 1983; Zinke et al., 2006), to increase (Zinke et al., 2006) or have no effect on (Sato et al., 1987; Sillito and Kemp, 1983) spontaneous activity, and to either decrease (Sato et al., 1987; Zinke et al., 2006) or increase (Sillito and Kemp, 1983; Murphy and Sillito, 1991) stimulus selectivity. It is difficult to relate our findings to the single-unit electrophysiological results for at least three reasons. First, the animal studies employed local administration of cholinergic drugs, while we administered donepezil systemically. Second, the electrophysiological studies typically tailored the properties of the visual stimulus so that it was nearly optimal for the recorded neuron. In contrast, our study involved presentation of a single stimulus, and this stimulus was optimal for only a small fraction of visual cortical neurons. Thus, the fMRI responses we recorded represent a population average of many neurons with a wide range of receptive field properties. Finally, our experiments were performed in awake behaving humans, while the electrophysiological studies were conducted in anesthetized animals. Many anesthetics strongly affect the activity of brain cholinergic systems (Backman et al., 2004), and the interactions between the effects of anesthetic and those of local administration of ACh are largely unknown.

Nonspecific Effects of Cholinergic Enhancement

Because the BOLD signal is a measure of blood oxygenation, changes in this signal could in principle be due to any combination of changes in neural activity, neurovascular coupling, and direct cholinergic effects on the vasculature. In fact, there is some evidence for cholinergic modulation of brain vasculature. Electrical stimulation of the nucleus basalis of Meynert, a cholinergic basal forebrain nucleus, increased cerebral blood flow in rat cortex, and this effect was blocked by systemic administration of ACh receptor antagonists (Biesold et al., 1989). Also, intravenous administration of nicotine has been reported to increase rCBF in human occipital cortex, both during rest and during performance of the perceptual maze test (Ghatan et al., 1998).

We performed a control experiment to assess the specificity of donepezil's effects on spatial spread and amplitude of visual responses. Donepezil had no effect on the amplitude of the breath holding BOLD response and reduced the temporal delay of this response in areas V1 and V3 (Figure 6). This decrease in temporal delay is unlikely to have affected our spatial spread measurements, as we defined the phase windows corresponding to positive and negative BOLD responses for each fMRI run based on the two-Gaussian fit of the pixel phase histograms.

Origin of Negative BOLD Signals

Many studies have shown that visual responses in early visual cortex consist of a positive BOLD response in the portions of visual cortical areas that retinotopically represent the stimulus locations, surrounded by a negative BOLD response in adjacent cortical regions (Bressler et al., 2007; Shmuel et al., 2002; Smith et al., 2000; Tootell et al., 1998). One possible explanation of negative BOLD responses is blood stealing, in which active cortex diverts oxygenated blood away from adjacent locations, resulting in a decrease in BOLD signal surrounding the stimulus response. However, combined electrophysiological and fMRI measurements in macaque early visual cortex have demonstrated that negative BOLD responses to visual stimulation are correlated with a decrease in neuronal firing rates in the same region (Shmuel et al., 2006). In addition, a visual stimulus restricted to one visual hemifield can cause a positive BOLD response in visual cortex contralateral to the stimulus and a negative BOLD response in the ipsilateral hemisphere (Smith et al., 2004; Tootell

et al., 1998). These results are not consistent with an explanation based on blood stealing, as the positive and negative BOLD regions represent adjacent visual field locations but are located in different hemispheres. The two regions are neurally connected by the corpus callosum, but they are served by largely independent vasculature. Thus, the available evidence suggests that in early visual cortex, negative BOLD responses in regions flanking the visual stimulus representation are likely to reflect reductions in neuronal firing rates.

In the present study, we observed a negative BOLD response to visual stimulation in cortical regions a few centimeters away from the positive BOLD response region (Figures 1 and 3 and Figure S2). This negative BOLD often extended beyond the eccentricities used to retinotopically define V1, V2, and V3 (11°, far beyond the 4.5° radius of the checkerboard stimulus annulus used to measure spatial spread). Surround suppression has been quantified for single neurons in macaque V1 that had receptive fields with eccentricities similar to those in our stimulus annulus (Ichida et al., 2007). In this study, some neurons exhibited inhibitory surrounds that extended more than 13° of visual angle away from the receptive field center. Surround suppression in V1 has been attributed to feedback connections from higher cortical areas, as single lateral connections in V1 are often not long enough to directly connect the cortical locations representing the suppressing surround stimulus with those representing the center stimulus (Angelucci et al., 2002; Cavanaugh et al., 2002). However, chains of lateral connections could potentially also mediate long-range suppression. In the present study, the relative contributions of lateral and feedback connections to the negative BOLD response and to the spatial spread of the positive BOLD response are unknown. Experiments in which spatial attention is used to manipulate feedback signals to early visual cortex will provide information regarding the effects of top-down inputs on spatial integration in early visual cortex.

Conclusions

We have demonstrated that cholinergic enhancement with donepezil reduces the spatial spread of excitatory visual responses in early visual cortex. Retinotopic visual cortical areas provide an excellent system for probing lateral spread of responses through intracortical connections. Pharmacological manipulation of brain cholinergic systems has been shown to affect performance on a wide variety of perceptual and cognitive tasks, and many of these effects can be accounted for by a model of cholinergic regulation of the balance between afferent inputs and lateral connections (Hasselmo and McGaughy, 2004). The specific contributions of reduced visual cortical spatial integration by ACh to visual perception are not yet known, but the available physiological data result in clear predictions. If cholinergic enhancement reduces the efficacy of lateral intracortical projections that connect separate locations in retinotopic visual field maps in early visual cortex, this should impair performance in tasks that strongly depend on integration across visual space, such as perceptual grouping or texture perception. On the other hand, tasks that require segmentation of spatial locations in the visual field, such as overcoming visual crowding or surround suppression, may show an improvement in performance following cholinergic enhancement.

Visual crowding results from excessive integration of stimuli presented in the peripheral visual field (Levi, 2008). In healthy humans, crowding is easily overcome by eye movements that bring the crowded stimuli into the central visual field. However, patients with macular degeneration suffer from degeneration of the portions of their retinae that represent the central visual field. Consequently, their entire visual field is crowded, resulting in severe impairments in reading, recognizing facial identity, and other important visual functions. The present results suggest that the cholinergic system may be a target for pharmacological treatment of the perceptual consequences of macular degeneration.

EXPERIMENTAL PROCEDURES

Subjects

Five healthy subjects participated in the study, all of whom had extensive experience as subjects in psychophysical and fMRI experiments. Two subjects were also authors of the study (subjects #1 and #4). All subjects provided written informed consent, and the experimental protocol was approved by the Committee for the Protection of Human Subjects at the University of California, Berkeley. Each subject participated in one MR session to acquire high-resolution whole-brain anatomical images, at least one retinotopic mapping fMRI session to define the boundaries of cortical areas V1, V2, and V3, and between three and five pharmacology sessions to determine the effects of cholinergic enhancement on visual responses in early visual cortex.

Pharmacology

Capsules containing either 5 mg donepezil (Aricept) or lactose placebo were prepared by the Drug Products Services Laboratory at the University of California, San Francisco. Donepezil is commonly used in the treatment of Alzheimer's disease, and 5 mg represents the lowest dose prescribed to patients. Subjects ingested either a donepezil or placebo capsule 3 hr before the beginning of the fMRI scanning session. The timing of capsule administration is based on the finding that peak plasma levels of donepezil are reached ~4 hr after oral administration at doses similar to the 5 mg dose used in our study (Rogers and Friedhoff, 1998). All experiments were conducted in a double-blind fashion. Pharmacology sessions were separated by at least 2 weeks to allow donepezil to be completely eliminated (the half life of donepezil is ~80 hr in humans [Rogers and Friedhoff, 1998]).

Visual Stimuli

Subject passively viewed an annulus containing a contrast-reversing checkerboard while maintaining fixation in the center of the annulus. The inner diameter of the annulus was 3° of visual angle, and the outer diameter was 9°. The pixel intensities within the checkerboard were sinusoidally modulated in space and time, with a spatial frequency of 2 cyc/° and a temporal frequency of 2.5 Hz. The stimulus contrast was 100%. Stimuli were presented on a gamma-corrected flat-panel LCD monitor (MultiSync 2110, NEC, Itasca, IL) that was electrically shielded to reduce fMRI artifacts due to radiofrequency noise. The monitor was viewed with an angled mirror positioned above the subject's eyes, and the viewing distance was 185 cm. The checkerboard annulus was presented for 9.6 s in block alternation with 9.6 s of a gray screen with the same mean luminance as the checkerboard. Each fMRI run consisted of 16 cycles of stimulus and gray screen, resulting in a total duration of 307.2 s for each run. The total numbers of runs and sessions for each participant are shown in Table 2. Subjects were instructed to continuously maintain fixation throughout the stimulus and gray screen periods. The stimulus protocol was written in MATLAB (The MathWorks, Inc., Natick, MA) using the Psychophysics Toolbox (Brainard, 1997; Pelli, 1997).

fMRI Data Acquisition

fMRI experiments were conducted with a 4-Tesla Varian INOVA MR scanner (Palo Alto, CA). A transmit/receive surface radiofrequency coil was used to maximize contrast-to-noise ratio in occipital cortex. Functional echo-planar images were acquired using a two-shot gradient-echo EPI sequence. The field

Table 2. Number of fMRI Sessions and Runs Completed by Each Participant

	Placebo			Donepezil		
Subject #	# Sessions	PV Runs	BH Runs	# Sessions	PV Runs	BH Runs
1	3	10	4	2	8	4
2	2	7	4	3	12	4
3	1	4	2	2	8	3
4	3	12	5	2	7	4
5	2	8	4	2	8	4

A single PV run represents ~5 min of passive viewing of the checkerboard annulus alternating with a blank screen. A single BH run represents ~6 min of alternation of breath holding with paced breathing.

of view was either 180 × 180 mm or 224 × 224 mm, and the matrix size was 64 × 64, resulting in an inplane voxel resolution of either 2.81 × 2.81 mm or 3.5 × 3.5 mm. The repetition time (TR) was 2.4 s, and the echo time (TE) was 28 ms. Twenty slices in coronal orientation were prescribed with slice thickness of 3 mm and a 0.3 mm interslice gap. A set of T1-weighted anatomical images that were coplanar with the EPI images was acquired at the beginning of every imaging session. In a separate session, a set of high-resolution T1-weighted whole-brain anatomical images was acquired for each subject to allow functional data to be combined across multiple scanning sessions.

fMRI Data Preprocessing

Each fMRI run began with a single blank period corresponding to one-half of a stimulus cycle (4 TRs, or 9.6 s for passive viewing runs; 10 TRs, or 24 s for breath holding runs). The data acquired during this blank period were not included in the analysis. Head movements were corrected using a 3D image registration algorithm (MCFLIRT; Jenkinson et al., 2002). The time series at each voxel were high-pass filtered to remove low-frequency noise (Smith et al., 1999; Zarahn et al., 1997). Finally, each voxel's time series was divided by its mean intensity to convert the data from arbitrary units to percentage signal modulation and to compensate for the decrease in mean image intensity as a function of distance from the surface coil.

Definition of Early Visual Cortical Area Boundaries

The boundaries of cortical areas V1, V2, and V3 were defined using well-established phase-encoded retinotopic mapping methods (DeYoe et al., 1996; Engel et al., 1994, 1997; Sereno et al., 1995). Stimuli were rotating checkerboard wedges with check size scaled according to the cortical magnification factor in human V1 (Slotnick et al., 2001). Although early visual cortical areas can be mapped with these stimuli in the absence of explicit attentional demands, we have found that many cortical areas contain topographic maps based on both stimulus-driven and top-down spatial attention signals (Silver et al., 2005). These sensory and attention maps are in correspondence in many visual cortical areas (Silver et al., 2005). To enhance signals in topographic areas during retinotopic mapping, subjects performed a difficult target detection task. The target could appear anywhere within the rotating wedge at unpredictable times. This encouraged subjects to continuously maintain spatial attention over the entire wedge. Subjects practiced the task in a behavioral testing room to determine their performance as a function of eccentricity, and the target sizes were scaled to insure that target detectability was equivalent at all wedge locations. In the scanner, stimuli were presented using MR-compatible goggles (Resonance Technology, Northridge, CA). The field of view used for retinotopic mapping was approximately 22° × 30° of visual angle.

Partitioning of Visual Cortical Areas into Positive and Negative BOLD Regions

For each subject, cortical gray matter voxels were segmented (Larsson, 2001). Each fMRI run consisted of 16 cycles of block alternation of checkerboard stimulus and blank screen. The cycle duration was 19.2 s, so the signal in visually responsive voxels should modulate with a frequency of 1/19.2 s = 0.0521 Hz. A 0.0521 Hz sinusoid was fit to the fMRI time course of each gray matter voxel in every run. The free parameters of the sinusoid fit were its amplitude, corresponding to the magnitude of the visual response, and its phase, corresponding to the delay in the fMRI response relative to the stimulus cycle. These fitting parameters were then spatially transformed onto computationally-flattened cortical patches.

For a given cortical area, the response phases exhibited a bimodal distribution, with one mode corresponding to a positive blood oxygenation level-dependent (BOLD) response to the stimulus (activity higher for stimulus than blank screen), and the other corresponding to a negative BOLD response (activity higher for blank screen than stimulus). This bimodal distribution could easily be observed in a histogram of the phase values for each pixel (Figure 1B and Figure S1). The histogram was fit with two Gaussians, one for positive BOLD and one for negative BOLD. The free parameters were the means, standard deviations (widths), and amplitudes (heights) of the Gaussians and a y-offset term that added a constant number of pixels to all response phases. Optimization was performed using a sequential nonlinear method, implemented as the function fminsearch in MATLAB. The fitting procedure was carried out separately for both hemispheres in each visual area and each fMRI run (consisting of sixteen stimulus cycles, or 307.2 s).

Hartigan's dip test (Hartigan and Hartigan, 1985) for unimodality was applied to the pixel histogram for each run, as implemented by Mechler and Ringach (2002) (Matlab code available at http://web.mac.com/darioringach/lab/Data.html). This tests the null hypothesis of a unimodal distribution and generates a confidence measure that a given distribution is multimodal. 487 out of a total of 504 histograms resulted in a Hartigan's dip test p value of less than 0.05, demonstrating that the signal-to-noise ratio for individual runs was sufficient to be able to identify separate pixel populations with positive and negative BOLD responses. fMRI runs that failed Hartigan's dip test were excluded from the analysis.

Breath Holding Task

Subjects performed block alternation of breath holding (24 s) and paced breathing (24 s, eight expiration/inspiration cycles). Subjects were cued to begin breath holding or to breathe in or out (for paced breathing) with text presented on the LCD monitor. Each fMRI run included seven cycles, for a total of 336 s per run. A sinusoid with a period of 48 s was fit to the fMRI time series for each voxel. The amplitude and phase of this sinusoid was computed for each voxel and separately averaged for both hemispheres in each cortical area. The total numbers of breath holding runs and sessions for each subject are shown in Table 2.

Eye Tracking Experiments

Eye position was recorded outside of the scanner in a behavioral testing room with an EyeLink 1000 system (SR Research, Osgoode, Ontario, Canada). A calibration was performed before each run to allow measurement of eye position in units of degrees of visual angle. Horizontal and vertical eye position were recorded at 1 kHz, and eye blinks were removed from the time series. Four subjects participated in one placebo session and one donepezil session. The experiments were conducted in a double-blind fashion, and the placebo or donepezil capsule was administered 3 hr before the beginning of the session, as in the fMRI experiments. Each subject participated in two 5 min runs for each session. The stimulus annulus was identical to that used in the fMRI experiment in size, spatial frequency, temporal frequency, and contrast. The timing of the block alternation (stimulus versus gray screen) and number of stimulus cycles were also equated in the fMRI and eye tracking experiments.

SUPPLEMENTAL DATA

The Supplemental Data include eight figures and can be found with this article online at http://www.neuron.org/supplemental/S0896-6273(08)00841-6.

ACKNOWLEDGMENTS

We thank Clare Gollnick for assistance with fMRI data analysis and Weston Pack for help with the eye position measurements. This work was supported by R01-MH63901 to M.D.

Accepted: September 19, 2008
Published: December 10, 2008

REFERENCES

Angelucci, A., and Bressloff, P.C. (2006). Contribution of feedforward, lateral and feedback connections to the classical receptive field center and extra-classical receptive field surround of primate V1 neurons. Prog. Brain Res. *154*, 93–120.

Angelucci, A., and Sainsbury, K. (2006). Contribution of feedforward thalamic afferents and corticogeniculate feedback to the spatial summation area of macaque V1 and LGN. J. Comp. Neurol. *498*, 330–351.

Angelucci, A., Levitt, J.B., Walton, E.J.S., Hupé, J.-M., Bullier, J., and Lund, J.S. (2002). Circuits for local and global signal integration in primary visual cortex. J. Neurosci. *22*, 8633–8646.

Backman, S.B., Fiset, P., and Plourde, G. (2004). Cholinergic mechanisms mediating anesthetic induced altered states of consciousness. Prog. Brain Res. *145*, 197–206.

Bentley, P., Husain, M., and Dolan, R.J. (2004). Effects of cholinergic enhancement on visual stimulation, spatial attention, and spatial working memory. Neuron *41*, 969–982.

Bentley, P., Driver, J., and Dolan, R.J. (2008). Cholinesterase inhibition modulates visual and attentional brain responses in Alzheimer's disease and health. Brain *131*, 409–424.

Biesold, D., Inanami, O., Sato, A., and Sato, Y. (1989). Stimulation of the nucleus basalis of Meynert increases cerebral cortical blood flow in rats. Neurosci. Lett. *98*, 39–44.

Brainard, D.H. (1997). The psychophysics toolbox. Spat. Vis. *10*, 433–436.

Bressler, D., Spotswood, N., and Whitney, D. (2007). Negative BOLD fMRI response in the visual cortex carries precise stimulus-specific information. PLoS ONE *2*, e410. 10.1371/journal.pone.0000410.

Cavanaugh, J.R., Bair, W., and Movshon, J.A. (2002). Nature and interaction of signals from the receptive field center and surround in macaque V1 neurons. J. Neurophysiol. *88*, 2530–2546.

DeAngelis, G.C., Freeman, R.D., and Ohzawa, I. (1994). Length and width tuning of neurons in the cat's primary visual cortex. J. Neurophysiol. *71*, 347–374.

DeYoe, E.A., Carman, G.J., Bandettini, P., Glickman, S., Wieser, J., Cox, R., Miller, D., and Neitz, J. (1996). Mapping striate and extrastriate visual areas in human cerebral cortex. Proc. Natl. Acad. Sci. USA *93*, 2382–2386.

Disney, A.A., Aoki, C., and Hawken, M.J. (2007). Gain modulation by nicotine in macaque V1. Neuron *56*, 701–713.

Engel, S.A., Rumelhart, D.E., Wandell, B.A., Lee, A.T., Glover, G.H., Chichilnisky, E.-J., and Shadlen, M.N. (1994). fMRI of human visual cortex. Nature *369*, 525.

Engel, S.A., Glover, G.H., and Wandell, B.A. (1997). Retinotopic organization in human visual cortex and the spatial precision of functional MRI. Cereb. Cortex *7*, 181–192.

Estermann, S., Daepp, G.-C., Cattapan-Ludewig, K., Berkhoff, M., Frueh, B.E., and Goldblum, D. (2006). Effect of oral donepezil on intraocular pressure in normotensive Alzheimer patients. J. Ocul. Pharmacol. Ther. *22*, 62–67.

Furey, M.L., Pietrini, P., and Haxby, J.V. (2000). Cholinergic enhancement and increased selectivity of perceptual processing during working memory. Science *290*, 2315–2319.

Ghatan, P.H., Ingvar, M., Eriksson, L., Stone-Elander, S., Serrander, M., Ekberg, K., and Wahren, J. (1998). Cerebral effects of nicotine during cognition in smokers and non-smokers. Psychopharmacology *136*, 179–189.

Gil, Z., Connors, B.W., and Amitai, Y. (1997). Differential regulation of neocortical synapses by neuromodulators and activity. Neuron *19*, 679–686.

Giocomo, L.M., and Hasselmo, M.E. (2007). Neuromodulation by glutamate and acetylcholine can change circuit dynamics by regulating the relative influence of afferent input and excitatory feedback. Mol. Neurobiol. *36*, 184–200.

Hartigan, J.A., and Hartigan, P.M. (1985). The dip test of unimodality. Annals of Statistics *13*, 70–84.

Hasselmo, M.E. (2006). The role of acetylcholine in learning and memory. Curr. Opin. Neurobiol. *16*, 710–715.

Hasselmo, M.E., and Bower, J.M. (1992). Cholinergic suppression specific to intrinsic not afferent fiber synapses in rat piriform (olfactory) cortex. J. Neurophysiol. *67*, 1222–1229.

Hasselmo, M.E., and McGaughy, J. (2004). High acetylcholine levels set circuit dynamics for attention and encoding and low acetylcholine levels set dynamics for consolidation. Prog. Brain Res. *145*, 207–231.

Hsieh, C.Y., Cruikshank, S.J., and Metherate, R. (2000). Differential modulation of auditory thalamocortical and intracortical synaptic transmission by cholinergic agonist. Brain Res. *880*, 51–64.

Hubel, D.H., and Wiesel, T.N. (1965). Receptive fields and functional architecture in two nonstriate visual areas (18 and 19) of the cat. J. Neurophysiol. *28*, 229–289.

Ichida, J.M., Schwabe, L., Bressloff, P.C., and Angelucci, A. (2007). Response facilitation from the "suppressive" receptive field surround of macaque V1 neurons. J. Neurophysiol. *98*, 2168–2181.

Jacobsen, L.K., Gore, J.C., Skudlarski, P., Lacadie, C.M., Jatlow, P., and Krystal, J.H. (2002). Impact of intravenous nicotine on BOLD signal response to photic stimulation. Magn. Reson. Imaging *20*, 141–145.

Jenkinson, M., Bannister, P., Brady, M., and Smith, S. (2002). Improved optimization for the robust and accurate linear registration and motion correction of brain images. Neuroimage *17*, 825–841.

Kawai, H., Lazar, R., and Metherate, R. (2007). Nicotinic control of axon excitability regulates thalamocortical transmission. Nat. Neurosci. *10*, 1168–1175.

Kim, D.-S., Ronen, I., Olman, C., Kim, S.-G., Ugurbil, K., and Toth, L.J. (2004). Spatial relationship between neuronal activity and BOLD functional MRI. Neuroimage *21*, 876–885.

Kimura, F., Fukuda, M., and Tsumoto, T. (1999). Acetylcholine suppresses the spread of excitation in the visual cortex revealed by optical recording: possible differential effect depending on the source of input. Eur. J. Neurosci. *11*, 3597–3609.

Larsson, J. (2001). Imaging vision: functional mapping of intermediate visual processes in man. PhD thesis, Karolinska Institutet, Stockholm, Sweden. ISBN 91-7349-090-3.

Levey, A.I., Kitt, C.A., Simonds, W.F., Price, D.L., and Brann, M.R. (1991). Identification and localization of muscarinic acetylcholine receptor proteins in brain with subtype-specific antibodies. J. Neurosci. *11*, 3218–3226.

Levi, D.M. (2008). Crowding – An essential bottleneck for object recognition: A mini-review. Vision Res. *48*, 635–654.

Li, T.-Q., Kastrup, A., Takahashi, A.M., and Moseley, M.E. (1999). Functional MRI of human brain during breath holding by BOLD and FAIR techniques. Neuroimage *9*, 243–249.

Logothetis, N.K., Pauls, J., Augath, M., Trinath, T., and Oeltermann, A. (2001). Neurophysiological investigation of the basis of the fMRI signal. Nature *412*, 150–157.

Mechler, F., and Ringach, D.L. (2002). On the classification of simple and complex cells. Vision Res. *42*, 1017–1033.

Mentis, M.J., Sunderland, T., Lai, J., Connolly, C., Krasuski, J., Levine, B., Friz, J., Sobti, S., Schapiro, M., and Rapoport, S.I. (2001). Muscarinic versus nicotinic modulation of a visual task: a PET study using drug probes. Neuropsychopharmacology *25*, 555–564.

Mesulam, M.-M. (2004). The cholinergic innervation of the human cerebral cortex. Prog. Brain Res. *145*, 67–78.

Metherate, R., and Ashe, J.H. (1993). Nucleus basalis stimulation facilitates thalamocortical synaptic transmission in the rat auditory cortex. Synapse *14*, 132–143.

Murphy, P.C., and Sillito, A.M. (1991). Cholinergic enhancement of direction selectivity in the visual cortex of the cat. Neurosci. *40*, 13–20.

Oldford, E., and Castro-Alamancos, M.A. (2003). Input-specific effects of acetylcholine on sensory and intracortical evoked responses in the "barrel cortex" *in vivo*. Neurosci. *117*, 769–778.

Pelli, D.G. (1997). The VideoToolbox software for visual psychophysics: transforming numbers into movies. Spat. Vis. *10*, 437–442.

Prusky, G.T., Shaw, C., and Cynader, M.S. (1987). Nicotine receptors are located on lateral geniculate nucleus terminals in cat visual cortex. Brain Res. *412*, 131–138.

Roberts, M.J., Zinke, W., Guo, K., Robertson, R., McDonald, J.S., and Thiele, A. (2005). Acetylcholine dynamically controls spatial integration in marmoset primary visual cortex. J. Neurophysiol. *93*, 2062–2072.

Roberts, M., Delicato, L.S., Herrero, J., Gieselmann, M.A., and Thiele, A. (2007). Attention alters spatial integration in macaque V1 in an eccentricity-dependent manner. Nat. Neurosci. *10*, 1483–1491.

Rogers, S.L., and Friedhoff, L.T. (1998). Pharmacokinetic and pharmacodynamic profile of donepezil HCl following single oral doses. Br. J. Clin. Pharmacol. *46* (*Suppl. 1*), 1–6.

Saad, Z.S., Ropella, K.M., DeYoe, E.A., and Bandettini, P.A. (2003). The spatial extent of the BOLD response. Neuroimage *19*, 132–144.

Sarter, M., Hasselmo, M.E., Bruno, J.P., and Givens, B. (2005). Unraveling the attentional functions of cortical cholinergic inputs: interactions between signal-driven and cognitive modulation of signal detection. Brain Res. Brain Res. Rev. *48*, 98–111.

Sato, H., Hata, Y., Masui, H., and Tsumoto, T. (1987). A functional role for cholinergic innervation to neurons in the cat visual cortex. J. Neurophysiol. *58*, 765–780.

Sceniak, M.P., Ringach, D.L., Hawken, M.J., and Shapley, R. (1999). Contrast's effect on spatial summation by macaque V1 neurons. Nat. Neurosci. *2*, 733–739.

Schon, K., Atri, A., Hasselmo, M.E., Tricarico, M.D., LoPresti, M.L., and Stern, C.E. (2005). Scopolamine reduces persistent activity related to long-term encoding in the parahippocampal gyrus during delayed matching in humans. J. Neurosci. *25*, 9112–9123.

Sereno, M.I., Dale, A.M., Reppas, J.B., Kwong, K.K., Belliveau, J.W., Brady, T.J., Rosen, B.R., and Tootell, R.B.H. (1995). Borders of multiple visual areas in humans revealed by functional magnetic resonance imaging. Science *268*, 889–893.

Shmuel, A., Yacoub, E., Pfeuffer, J., Van de Moortele, P.-F., Adriany, G., Hu, X., and Ugurbil, K. (2002). Sustained negative BOLD, blood flow and oxygen consumption response and its coupling to the positive response in the human brain. Neuron *36*, 1195–1210.

Shmuel, A., Augath, M., Oeltermann, A., and Logothetis, N.K. (2006). Negative functional MRI response correlates with decreases in neuronal activity in monkey visual area V1. Nat. Neurosci. *9*, 569–577.

Sillito, A.M., and Kemp, J.A. (1983). Cholinergic modulation of the functional organization of the cat visual cortex. Brain Res. *289*, 143–155.

Silver, M.A., Ress, D., and Heeger, D.J. (2005). Topographic maps of visual spatial attention in human parietal cortex. J. Neurophysiol. *19*, 9480–9496.

Slotnick, S.D., Klein, S.A., Carney, T., and Sutter, E.E. (2001). Electrophysiological estimate of human cortical magnification. Clin. Neurophysiol. *112*, 1349–1356.

Smith, A.M., Lewis, B.K., Ruttimann, U.E., Ye, F.Q., Sinnwell, T.M., Yang, Y., Duyn, J.H., and Frank, J.A. (1999). Investigation of low frequency drift in fMRI signal. Neuroimage *9*, 526–533.

Smith, A.T., Singh, K.D., and Greenlee, M.W. (2000). Attentional suppression of activity in the human visual cortex. Neuroreport *11*, 271–277.

Smith, A.T., Williams, A.L., and Singh, K.D. (2004). Negative BOLD in the visual cortex: evidence against blood stealing. Hum. Brain Mapp. *21*, 213–220.

Sperling, R., Greve, D., Dale, A., Killiany, R., Holmes, J., Rosas, H.D., Cocchiarella, A., Firth, P., Rosen, B., Lake, S., et al. (2002). Functional MRI detection of pharmacologically induced memory impairment. Proc. Natl. Acad. Sci. USA *99*, 455–460.

Stillman, A.E., Hu, X., and Jerosch-Herold, M. (1995). Functional MRI of brain during breath holding at 4T. Magn. Res. Imag. *13*, 893–897.

Tootell, R.B.H., Mendola, J.D., Hadjikhani, N.K., Liu, A.K., and Dale, A.M. (1998). The representation of the ipsilateral visual field in human cerebral cortex. Proc. Natl. Acad. Sci. USA *95*, 818–824.

Zarahn, E., Aguirre, G.K., and D'Esposito, M. (1997). Empirical analyses of BOLD fMRI statistics. I. Spatially unsmoothed data collected under null-hypothesis conditions. Neuroimage *5*, 179–197.

Zinke, W., Roberts, M.J., Guo, K., McDonald, J.S., Robertson, R., and Thiele, A. (2006). Cholinergic modulation of response properties and orientation tuning of neurons in primary visual cortex of anaesthetized Marmoset monkeys. Eur. J. Neurosci. *24*, 314–328.